Measurement Notes
Note 41
February 1993

ELLIPTICUS FERRITE/RESISTIVE LOADING

Gary D. Sower
EG&G Special Projects

Donald P. McLemore
KSC, Dikewood Division

William D. Prather
Phillips Laboratory

ABSTRACT

Resistively-loaded antennas are used to control the wave impedance of the electromagnetic field in the working volume; the ratio of the electric to the magnetic field over some specified frequency bandwidth is made to be equal to some desired value, usually that of the free-space impedance. In the large diameter antennas (HPD, TES, MEMPS) resistor modules are used. In a thin-wire antenna such as ELLIPTICUS, where the drive cable carrying the signal to the antenna feed also serves as the antenna conductor, this type of resistive loading is not possible.

The desired resistance is obtained by placing ferrite beads over the cable, and utilizing their properties as radio-frequency chokes. The ferrite presents a complex impedance (inductance plus loss) to the current flow on the outside of the cable, which is in series with the natural impedances such as radiation resistance.

The impedance of the ferrite is dominated at lower frequencies by the real component of its permeability, which gives the inductance that is usually the parameter of consideration. At the higher frequencies of interest here, however, the losses of the ferrite, due to the imaginary part of the permeability, present the larger impedance component. Both of these permeability components are highly frequency dependant, and thus would present a frequency-dependant impedance to currents on the antenna.

The real part (resistance) of the impedance can be made to have a much flatter frequency response by putting a secondary winding on the ferrite bead with the proper values of resistance and inductance. This procedure has the added benefit of greatly reducing the imaginary part (inductance), giving a nearly pure resistance. It is accomplished simply by connecting one or more resistors around the bead cross section, with the parallel value of the resistors in parallel with the unloaded ferrite resistance giving the desired resistance value. The number of resistors used controls the load inductance, which in parallel with the ferrite impedance governs the high-frequency antenna performance.

I. INTRODUCTION

The resistive loading of the ELLIPTICUS antenna by means of ferrite beads with load resistors is described [1]. The desired resistance is calculated to be **14.4 Ω/m**. The theory of a toroidal core of ferrite material is presented. The insertion impedance presented to the antenna by a ferrite toroid with a load impedance consisting of a resistor and its associated lead inductance is derived. A method to measure the insertion impedance of the toroid, either with or without the load resistor, is developed. Measurement data for different ferrite materials are presented, including different load resistance inductance values. Comparison of the measured data is shown to be in agreement with the theory. Samples of the actual toroids to be used on the antenna were obtained. Characterization of these samples is performed, as is the optimization of the load impedance to give the desired antenna impedance. The result is that only one type of ferrite material needs to be used on ELLIPTICUS to cover the frequency range of interest, 100 kHz to 1000 MHz; the original concept of using low-frequency material in conjunction with high-frequency material is not necessary. Only the low-frequency ferrite toroids are needed. One toroid will be fastened over the antenna coax every **50 cm**, with a **10 ohm** load consisting of **four 39 Ω** resistors equally spaced around it. This resistance in parallel with the ferrite impedance gives about **7 ohms** for each toroid. For the first few meters away from the drive point, one toroid will be placed every **25 cm**, with an insertion impedance of **3.5 ohms**. There will be about **250** total toroid assemblies on the antenna, **125** on each side.

II. ANTENNA RESISTIVE LOADING

ELLIPTICUS is designed to perform in a manner as nearly identical to HPD (ATHAMAS I) as practical: Approximate rather than exact solutions are used to give a ratio of electric to magnetic fields identically equal to free-space impedance at the center of the ellipse for low-frequency fields. These use the resistive loading calculations based on a circular torus, instead of the exact calculations for the elliptical shape.

The resistive loading of the HPD antenna, R_0 ohms per meter, is given by the formula [2,3]:

$$R_0 = 120\pi \left[\ln\left(8 \frac{a_{eff}}{b_{eff}} \right) - 2 \right], \qquad (1)$$

where a_{eff} = **47.4 m** is the radius of a circle with the same area as the antenna ellipse and b_{eff} = **1.81 m** is the effective radius of a solid cylinder as represented by the 12 wires of the antenna. This gives **1260 Ω** for the resistance of the full ellipse, **630 Ω** for the full HPD antenna, or **315 Ω** for each side of the antenna. In actuality, HPD is constructed with **305 Ω** on each side: It appears that one resistor station (10.2 Ω) was omitted from the antenna during several rounds of design iterations. The resulting resistance error is one part in 31 (0.3 dB) and not significant to the accuracy to which we can make ELLIPTICUS mimic the HPD.

The resistive loading of the ELLIPTICUS antenna is easily changed merely by changing FEB spacing or resistor loads. At any time in the future it will thus be a simple task to modify the loading to actually obtain a true free-space field ratio, or any other desired experimental configuration.

We use the same formula for ELLIPTICUS with the antenna elliptical geometry of two-thirds that of HPD, giving a_{eff} = 31.6 m, and b = .188" x .0254 m/" the radius of the 3/8" Heliax coaxial cable. This gives the resistance of the full ellipse of 3348 Ω, which is 837 Ω for each side of the antenna. The length of each of the coaxial cables forming the ELLIPTICUS antenna is approximately
57.3 m, so the desired resistive loading is about 14.6 Ω/m.

III. FERRITE BEAD LOADING

The resistive loading of ELLIPTICUS will be achieved by placing ferrite beads (FEB) over the jacket of the coaxial cable of the antenna. Each FEB presents a series impedance Z_B to the electrical current running over the outside of the coax, which consists of a real (resistive) part and an imaginary (reactive) part, both of which are frequency dependant as:

$$Z_B(\omega) = R_B(\omega) + jX_B(\omega) \quad . \tag{2}$$

A phenomenological description of magnetic materials [4] shows that the complex susceptibility of the material is given by:

$$\chi^* = \chi' - j\chi'' \quad . \tag{3}$$

The real and imaginary parts are not independent, but are functions of each other according to the Kramers-Kronig relations:

$$\chi'(\omega) = \frac{2}{\pi}\int_0^\infty \frac{\omega' \chi''(\omega')}{(\omega'^2 - \omega^2)}\, d\omega' \quad , \tag{4}$$

$$\chi''(\omega) = -\frac{2}{\pi}\int_0^\infty \frac{\omega \chi'(\omega')}{(\omega'^2 - \omega^2)}\, d\omega' \quad . \tag{5}$$

This relation is a result of the Hilbert transform pairs [5,6]. Thus, if either term is known over its entire spectrum, the other term is exactly determined to within an additive constant. At zero frequency the second term (χ") becomes identically zero and the first term becomes the static susceptibility χ_0, which gives the unique solution of (4) and (5) with the constants of integration equal to zero.

IV. TOROIDAL CORE

When a toroidal core of magnetic material is placed around a wire, it becomes an impedance to current flowing in the wire because energy is required to establish the magnetic flux in the core and because of energy dissipation in the core. Power losses generated within the core by the changing magnetic field may be represented by equivalent loss resistances [7]. These power losses are due to eddy currents and hysteresis losses, which may be represented by the equivalent eddy current loss resistance R_E and the equivalent hysteresis resistance R_H. The two equivalent resistances must be in parallel to give the correct power losses, which is just the loss resistance R_B.

At low frequencies, the equivalent hysteresis resistance is proportional to the frequency and the eddy current equivalent resistance to the resistivity of the material. For very high resistivity ferrite, the eddy current equivalent resistance becomes very large and can be neglected.

Figure 1 shows the geometry for a toroidal core of rectangular cross section placed coaxially around a wire which carries a current $I(\omega)$.

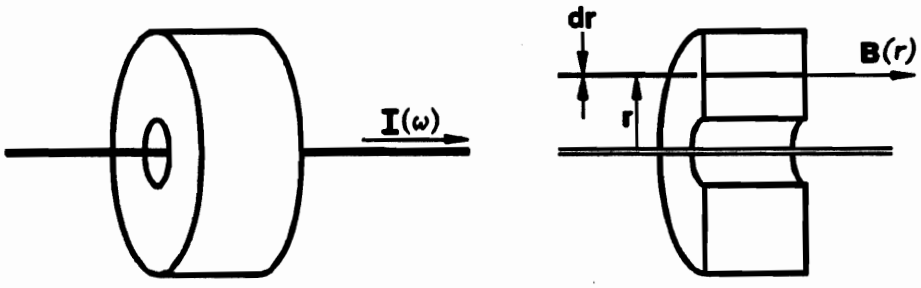

Figure 1. Torroidal bead with rectangular cross section.

The flux density **B(r)** in the core at radius **r** from the axis is:

$$B(r) = \mu_0 (1 + \chi^*) H(r) = \mu_0 (1 + \chi^*) \frac{I(\omega)}{2\pi r} \quad . \tag{6}$$

The total magnetic flux Φ in the core is obtained by integrating **B(r)** over the length **d** and radius **a** to **b**:

$$\Phi = d \int_a^b B(r)\, dr = \left[\frac{\mu_0}{2\pi}\, d\, \ell n\left(\frac{b}{a}\right)\right] (1 + \chi^*)\, I(\omega) \quad . \tag{7}$$

The total series impedance $\mathbf{Z_B = R_B + jX_B}$ presented to the current by the toroid can therefore be given by the complex susceptibility:

$$Z_B = j\omega \frac{\Phi}{I} = j\omega \left[\frac{\mu_0}{2\pi}\, d\, \ell n\left(\frac{b}{a}\right)\right] (1 + \chi' - j\chi'') \quad . \tag{8}$$

The real and imaginary parts are then separated as:

$$R_B(\omega) = \omega \left[\frac{\mu_0}{2\pi}\, d\, \ell n\left(\frac{b}{a}\right)\right] \chi''(\omega) \quad , \tag{9}$$

$$X_B(\omega) = \omega\, L_B(\omega) = \omega \left[\frac{\mu_0}{2\pi}\, d\, \ell n\left(\frac{b}{a}\right)\right] [1 + \chi'(\omega)] \quad . \tag{10}$$

The inductance of the toroid is defined in terms of the real part of the susceptibility to be:

$$L_B(\omega) = \Re\left(\frac{\Phi}{I}\right) = \left[\frac{\mu_0}{2\pi}\, d\, ln\left(\frac{b}{a}\right)\right]\, [1 + \chi'(\omega)] \ . \qquad (11)$$

The term in brackets, which has occurred in all of the above impedance equations, is the inductance of an empty cavity of the same dimensions as the toroidal core; it is the free-space contribution to the permeability:

$$L_0 = \left[\frac{\mu_0}{2\pi}\, d\, ln\left(\frac{b}{a}\right)\right] \ . \qquad (12)$$

The resistive term may also be calculated from the power dissipated in the core per unit volume:

$$p(\omega) = \mu_0 \frac{\omega}{2}\, \chi''(\omega)\, H(\omega)^2 \ . \qquad (13)$$

The total power dissipated within the core **P(ω)** is obtained by integrating over the volume of the core where **dV = d 2πr dr**:

$$P(\omega) = \int_a^b \frac{\mu_0 \omega}{2} \chi''(\omega)\, I(\omega)^2 \frac{d}{2\pi r} dr = \frac{\omega}{2}\left[\frac{\mu_0}{2\pi}\, d\, ln\left(\frac{b}{a}\right)\right] \chi''(\omega)\, I(\omega)^2 \ . \qquad (14)$$

The total RMS power dissipated as heat in $\mathbf{R_B}$ is:

$$P(\omega) = \frac{1}{2}\, I(\omega)^2\, R_B(\omega) \ . \qquad (15)$$

Equating the dissipated power in **(14)** and **(15)** yields the verification of **(9)**.

The dissipation of the magnetic material, being in quadrature phase with its inertia, is a classic case of **relaxation**, in which a unit step excitation decays exponentially with a characteristic time constant τ. For a material with a single relaxation time $\tau = 1/\omega_0$ where ω_0 is on the order of the Larmor precession frequency, the susceptibility reduces to the **Debye** relaxation equation:

$$\chi^*(\omega) = \chi_0 \frac{1 - j\omega\tau}{1 + \omega^2\tau^2} = \chi_0 \frac{\omega_0^2 - j\omega\omega_0}{\omega_0^2 + \omega^2} \ . \qquad (16)$$

This equation, and linear combinations of it, obey the **Kramers-Kronig** relations. The impedance terms given by **(10)** and **(11)** then become:

$$R_S(\omega) = \left[\frac{\mu_0}{2\pi}\, d\, \ell n\left(\frac{b}{a}\right)\right] \chi_0 \frac{\omega^2\, \omega_0}{\omega^2 + \omega_0^2}\,, \qquad (17)$$

$$\omega L_S(\omega) = \left[\frac{\mu_0}{2\pi}\, d\, \ell n\left(\frac{b}{a}\right)\right] \omega \left[1 + \frac{\chi_0\, \omega_0^2}{\omega^2 + \omega_0^2}\right]. \qquad (18)$$

These curves are plotted in **Figure 2** for a hypothetical ferrite bead with the parameters and the dimensions shown. For a homogeneous mixture of different magnetic materials with different static susceptibilities and relaxation times, the properties of each part add proportionally to give the properties of the whole.

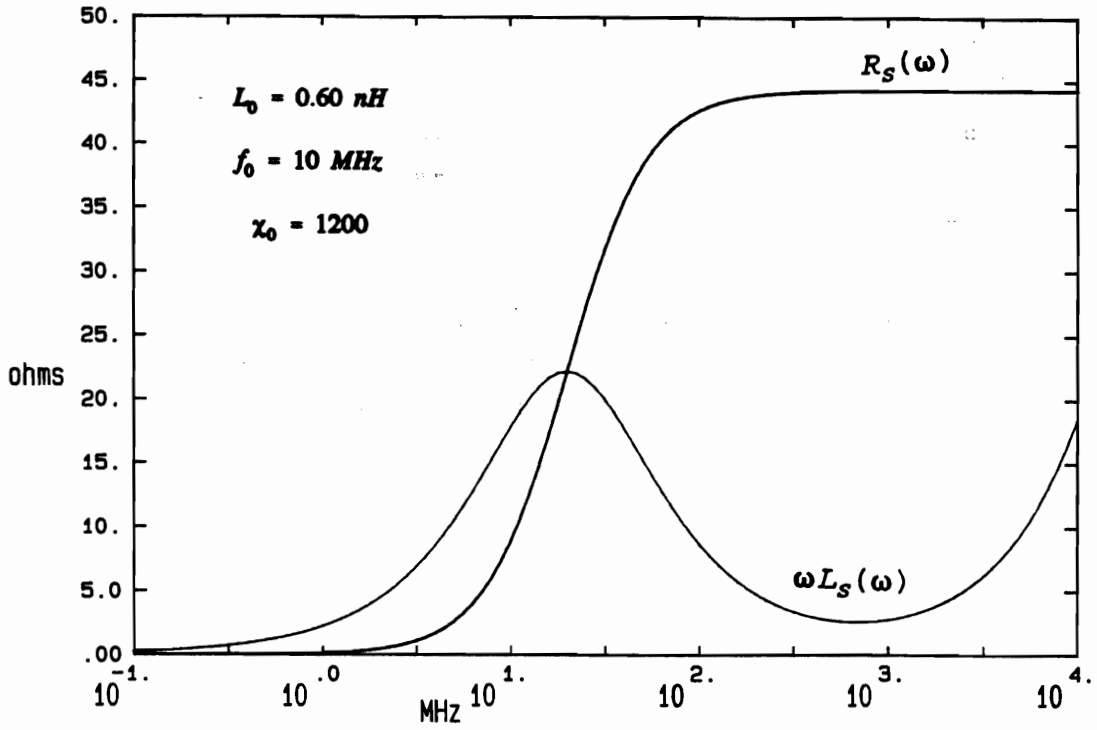

Figure 2. FEB impedance for Debye relaxation equation.

V. TRANSFORMER

When a single-turn secondary winding with a load impedance Z_L is put on the FEB, it becomes a transformer and the simplified equivalent circuit of **Figure 3** is applicable, where we have ignored stray impedances such as inter-winding capacitance, leakage flux, etc.

The use of the toroidal inductor as the broadband transformer core has several distinct advantages over other shapes. It has the maximum inductance per unit volume. Leakage flux is minimized, especially if a coaxial

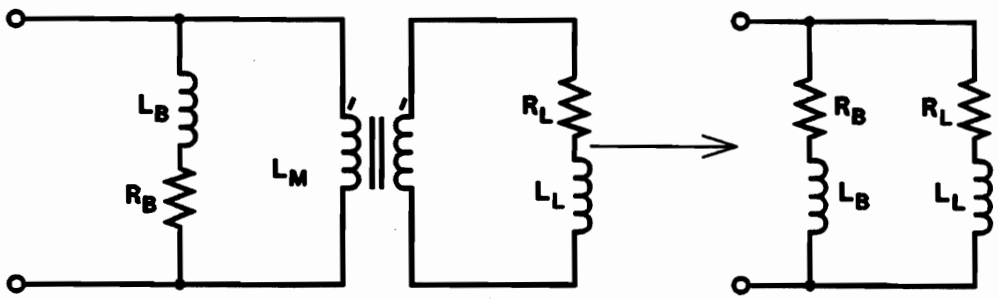

Figure 3. Equivalent Circuit of Impedance of FEB with Load Impedance.

winding geometry is used, and shielding requirements are reduced. The inductance of the toroid and its temperature stability are directly related to the average incremental permeability of the core material.

For the ELLIPTICUS loading [1], the load impedance will consist of one or more resistors in parallel around the core, giving a load impedance of the (parallel combination) resistance in series with the lead inductance:

$$Z_L = R_L + j\omega L_L \ . \tag{19}$$

The total impedance presented to the current on the antenna is:

$$Z_T = R_T + jX_T = \frac{(R_L + j\omega L_L)\ (R_B + j\omega L_B)}{(R_L + j\omega L_L) + (R_B + j\omega L_B)} \ . \tag{20}$$

The real part of this expression is a function of each of the four components of the equivalent circuit, as is the imaginary part.

VI. MEASUREMENTS

There are two frequency regimes of importance for measuring the characteristics of the FEB: The first is the low-frequency range where the bead and test fixture are both **electrically short**, where the longest dimensions, including dielectric effects, are much shorter than the shortest wavelength of interest. In this case lumped electrical circuit parameters can be used, and the measurements are readily carried out without significant error. Techniques for this regime can be extended into the gigahertz range by making the FEB small and using coaxial test fixtures which are the same length as the bead.

The second range occurs when significant fractions of wavelengths, or many wavelengths, occur within the ferrite material and the test fixture. In this case transmission line measurements and analysis must be used, with great care taken to minimize stray impedances, impedance discontinuities, phase errors, and the like. It is also possible to measure the complex permittivity [8].

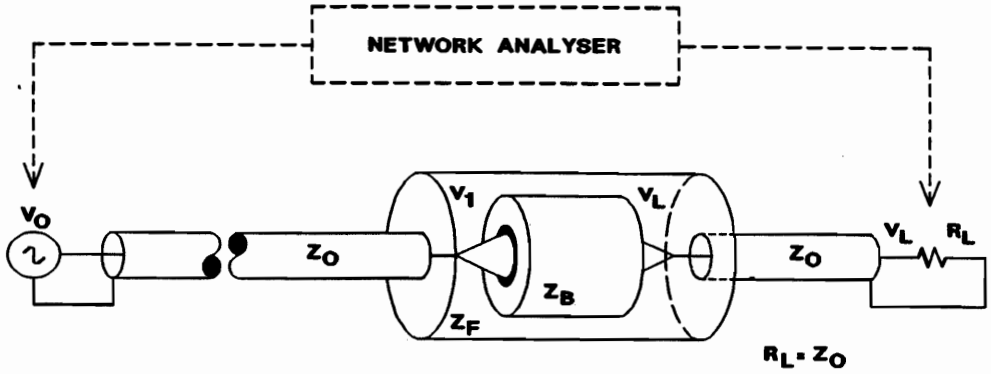

Figure 4. FEB Characterization System.

The first method, for electrically short measurements is the one used here. The measurement system of Figure 4 is used to characterize the FEB. A coaxial test fixture was made in which the FEB is placed. When the test fixture is empty, the voltage signal at the output is approximately equal to that at the input. With the FEB in the fixture, its impedance, with or without a load,

$$Z_T = R_T + jX_T \ , \tag{21}$$

is added to that of the test fixture, giving:

$$Z = Z_T + Z_F = Z_T + Z_0 \ . \tag{22}$$

The voltage across this impedance is that transmitted across the transmission line discontinuity:

$$V_1 = V_0 \frac{2Z}{Z + Z_0} = 2V_0 \frac{Z_B + Z_0}{Z_B + 2Z_0} \ . \tag{23}$$

The voltage signal across the load (recording instrument) with the FEB is designated by V_B, and is:

$$V_B \equiv V_L = V_1 \frac{Z_0}{Z} = V_0 \frac{2Z_0}{Z_T + 2Z_0} \ . \tag{24}$$

The impedance of the FEB is then obtained from the two measurements of the voltage as:

$$Z_T(\omega) = 2Z_0 \left(\frac{V_0(\omega)}{V_B(\omega)} - 1 \right) . \tag{25}$$

The real and imaginary parts of the impedance are then:

$$R_T(\omega) = 2 Z_0 \left[\Re\left(\frac{V_0(\omega)}{V_B(\omega)} \right) - 1 \right], \qquad (26)$$

$$X_T(\omega) = \omega L_T(\omega) = 2 Z_0 \, \Im\left(\frac{V_0(\omega)}{V_B(\omega)} \right). \qquad (27)$$

VII. TEST RESULTS

Measurements have been made on small ferrite beads using the electrically short technique. **Figure 5** shows the data obtained for one type of ferrite material (CMD5005) made by Ceramic Magnetics. The number T502525T gives the toroid dimensions as: Toroid, .50 inch O.D., .25 inch I.D., .25 inch long, Tumbled. The small oscillations at the upper frequencies are due to reflections within the ferrite and the test fixture, which was not matched to the characteristic impedance of the system. **Figure 6** is the data for another type of ferrite from the same manufacturer. It is readily apparent that the properties of these two materials are quite different. The material of **Figure 5** is a high-frequency ferrite which has been used extensively in instrumentation baluns, etc. It is a nickel-zinc ferrite with an initial permeability of 1500 and a very high resistivity of 10^9 ohm-cm. It appears to have two relaxation frequencies, at about 2 MHz and 25 MHz.

The material of **Figure 6** is a manganese-zinc ferrite with a large initial permeability of 9500 and a very low resistivity of only 35 ohm-cm. This material appears to have two relaxation frequencies at 1 MHz and 2.5 MHz, with an "anti-relaxation" at 8 MHz. This anti-resonance seems to be typical of the Mn-Zn ferrites, and may be due to the low resistivity of the material which gives large eddy currents - further research into these properties is desirable, but not at this time.

Resistive loading of the FEB of **Figure 5** is shown in **Figure 7**. Four values of resistance are presented, along with the unloaded FEB. As the resistance is lowered the real part of the total impedance decreases, flattens, and extends to lower frequency. The imaginary part is seen to also decrease, with its peak moving to significantly lower frequency. Above the peak, its magnitude decreases significantly with respect to that of the real component. This material can be made to give a good total impedance for frequencies above 1 MHz.

The increase of the imaginary component at high frequency may be due to the inductance of the load. **Figure 8** shows this FEB with a [nearly] constant resistance and varying inductance: these curves do not support the above hypothesis - more data will be presented later on this subject.

Figure 9 shows the resistive loading of the low-frequency FEB. The same general comments apply as for the other ferrite, except that the useful frequency extends to 100 kHz. It would seen that this material by itself (or

a similar material) will give the desired ELLIPTICUS antenna loading, without having to also us the high-frequency ferrite.

VIII. CORRELATION WITH THEORY

We can approximate the ferrite material of **Figure 5** by a summation of two single relaxation time Debye equations, one with a relaxation frequency of 2 MHz and the other of one-third the magnitude at 25 MHz, **Figure 10**. **Figures 11-14** present the analytical data for various load impedances: The resistance is varied from zero to a large value. Three values of inductance are used in each figure, the first two being representative values for single or multiple parallel resistor leads. The smallest inductance value is about the minimum value possible, that for an inductive toroidal cavity that just enclosed the FEB. The figures for the appropriate resistor values show excellent agreement with the measured data of **Figure 7**, at least for the lower inductance values. **Figure 8** is now seen to be reasonably compatible with the theory, where the inductance variation is not very apparent below 200 MHz.

The low-frequency ferrite of **Figure 6** is approximated by the linear superposition of three Debye equations: the first at one MHz, the second of three times the amplitude at 1.5 MHz, and the third of opposite phase (negative) at 4.5 MHz with amplitude 0.18, **Figure 15**. **Figures 16-19** give the analytical data for the various load impedances. Again, excellent agreement is seen between experiment and theory.

IX. ANTENNA TOROIDS

Samples of ferrite toroids of materials similar to those measured above were obtained from Amidon Associates in the size to be used on the ELLIPTICUS antenna: FB77-1024 and FB43-1020, both with OD = 1.00" and ID = .50" and lengths of about .850" and 1.120", respectively. A test fixture was made for these toroids. One-quarter watt resistors were used for loads. **Figure 20** shows the impedance of the FB43 material, in a length of 1.12". It is a slightly higher frequency material than is the CMD5005, with perhaps a single relaxation frequency at 30 MHz.

Figure 21 is the impedance of the 0.850" long FB77 material. It is similar to the MC25 material, but again with probably a single positive relaxation frequency. Using a baseline configuration of two toroids per meter on the ELLIPTICUS antenna gives a desired real component of impedance of about **7 ohms**. The required resistive loading in parallel with the **17-28 ohms** of the FEB is then about **10 ohms**. **Figure 22** shows the achieved insertion impedance resulting from four configurations of 10 ohm loading, using Allen Bradley 1/4 watt resistors with the leads of each wrapped around the cross section of the toroid and soldered together as shown in **Figure 23**. It appears that four **39 ohm** resistors in parallel give the optimum performance, especially at the high frequencies. Above about 100 MHZ we expect the radiation efficiency of the antenna drive to add a significant radiation resistance to the antenna, which will add to the shown FEB resistance - the high frequencies radiate away from the drive point and do not propagate down the antenna, and thus do not need to be terminated. Only the FB77 toroids are required to give the desired ELLIPTICUS performance.

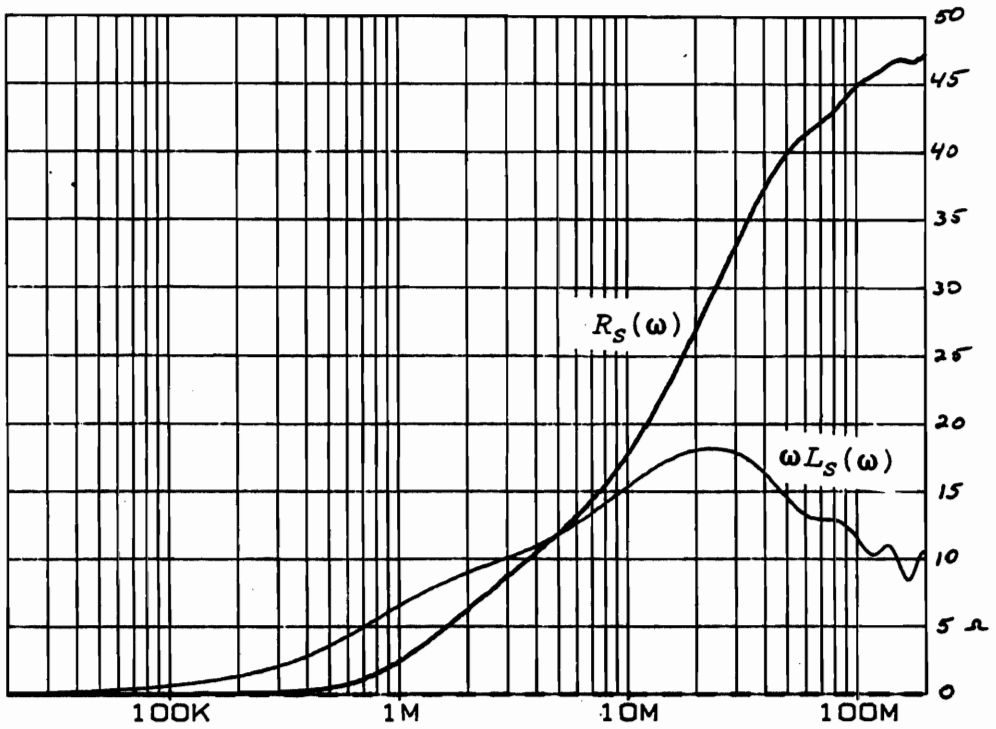

Figure 5. Real and Imaginary Impedances of CMD5005 T502525T FEB.

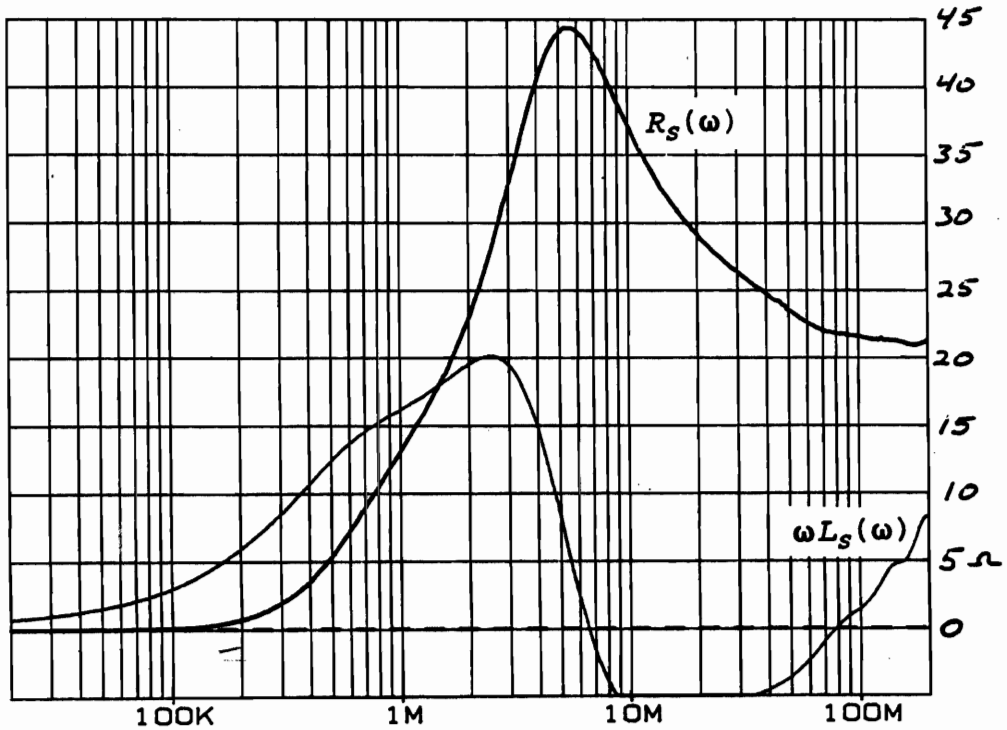

Figure 6. Real and Imaginary Impedances of MC25 T502825T FEB.

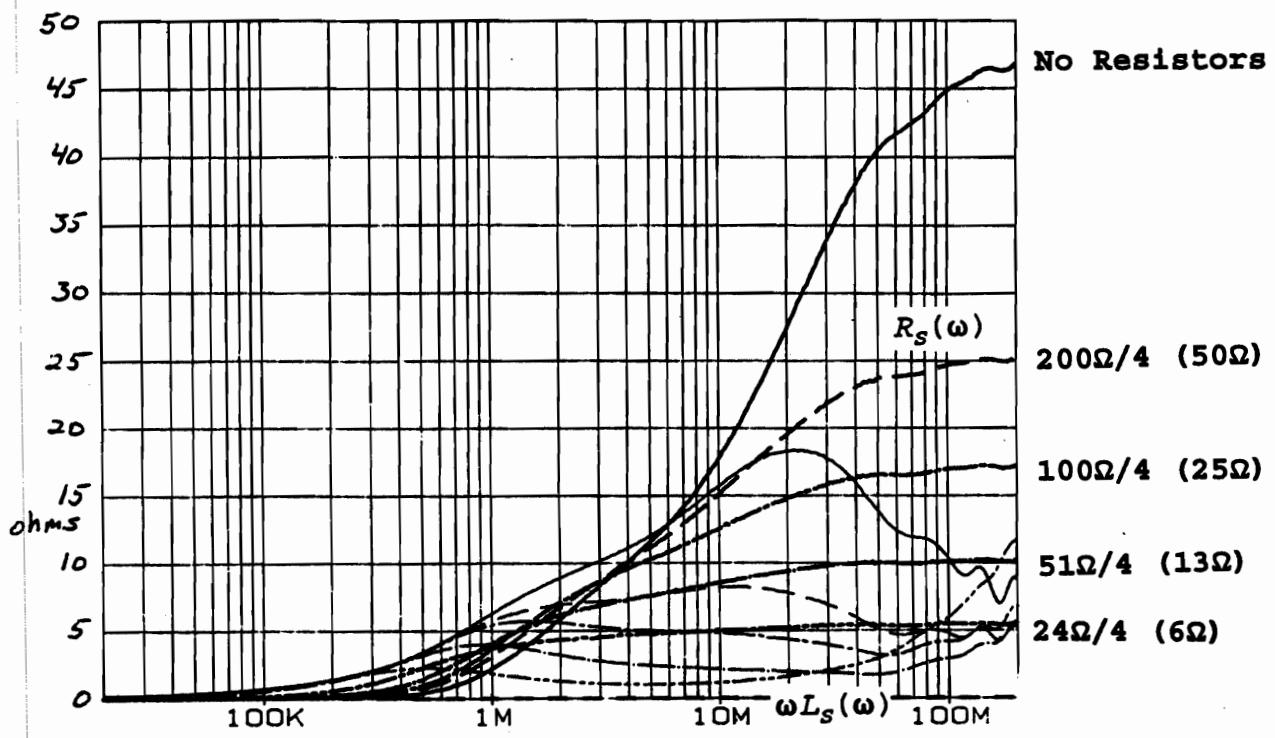

Figure 7. **Loading of CMD5005 T502525T Toroid with <u>FOUR</u> Parallel Resistors: Same Inductance, Varying Resistance.**

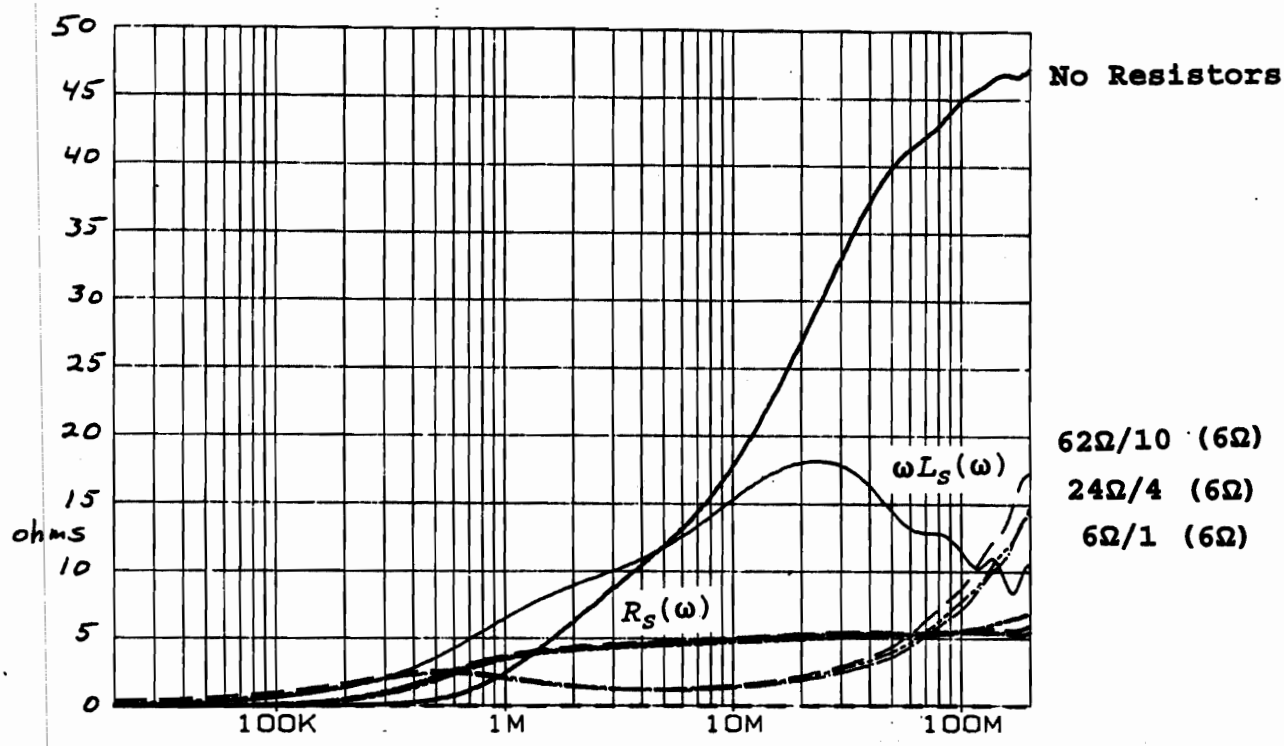

Figure 8. **Loading of CMD5005 T502525T Toriod with Parallel Resistors: Varying Inductance, Equal <u>6 OHM</u> Resistance.**

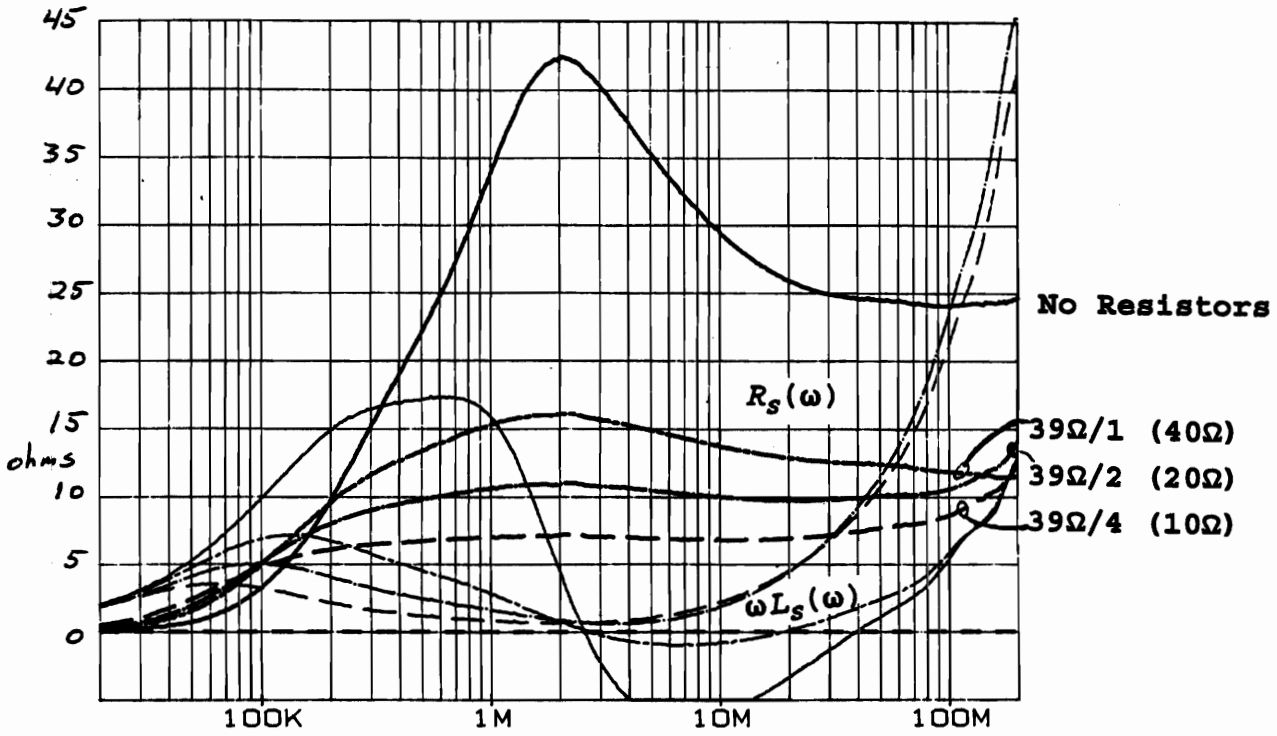

Figure 9. **Loading of MC25 T502825T Toroid with Parallel Resistors: Varying resistance and Inductance with 39 OHM Resistors.**

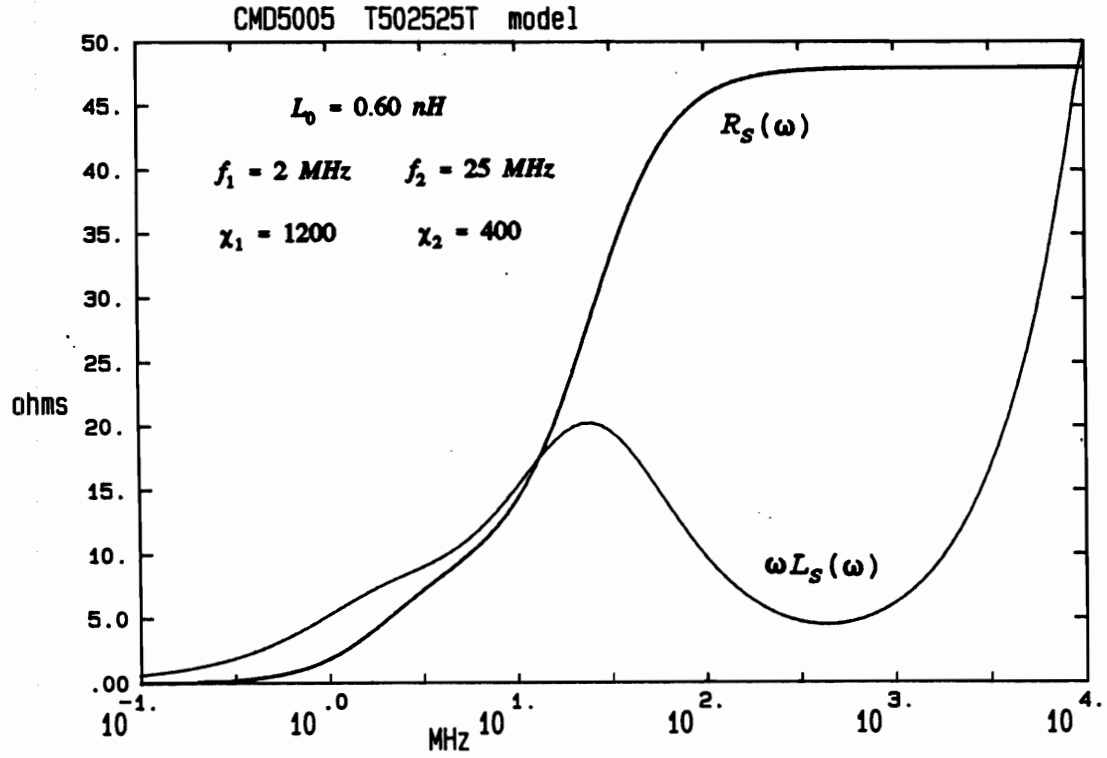

Figure 10. Analytical Model of CMD5005 T502525T FEB.

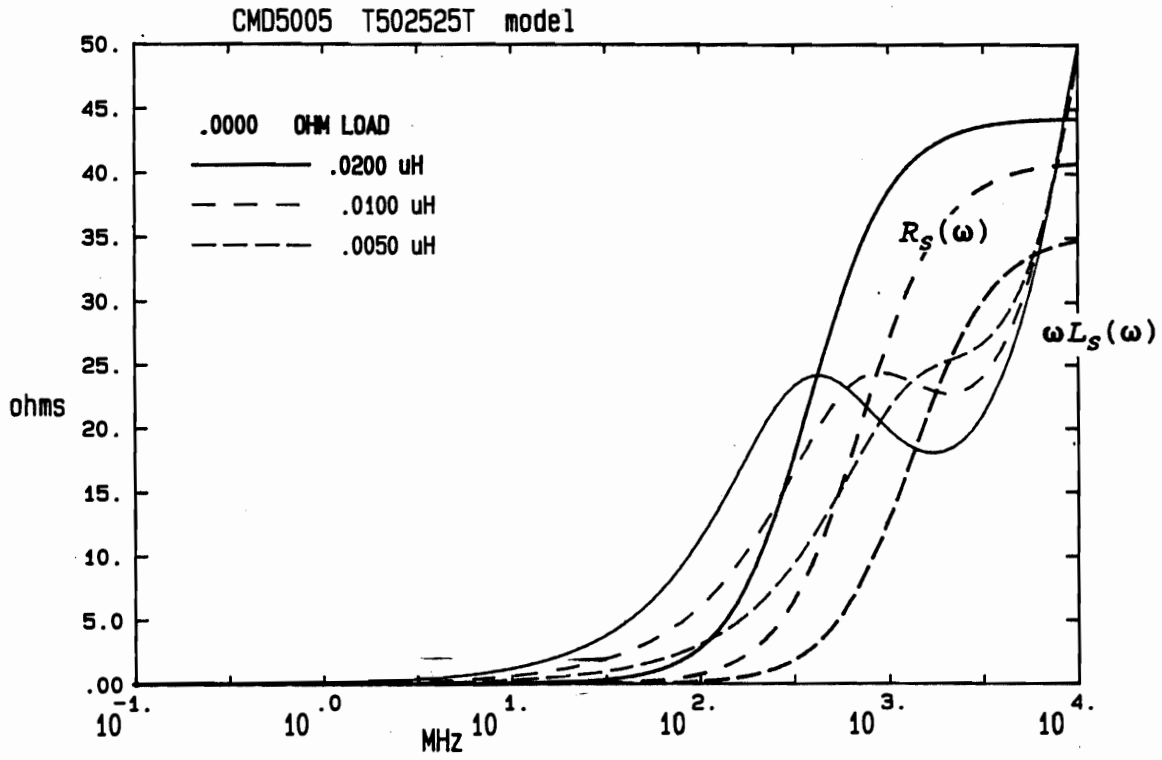

Figure 11. Analytical Model of CMD5005 T502525T FEB - short.

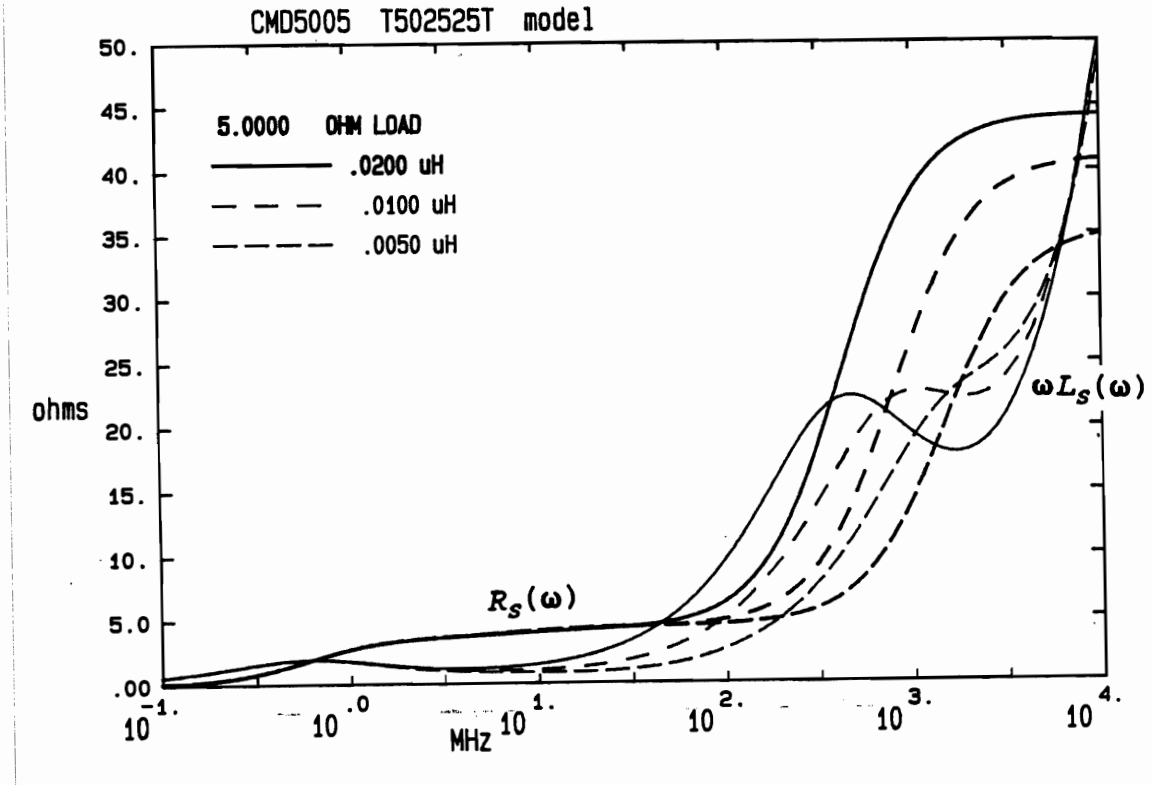

Figure 12. Analytical Model of CMD5005 T502525T FEB - 5 ohm.

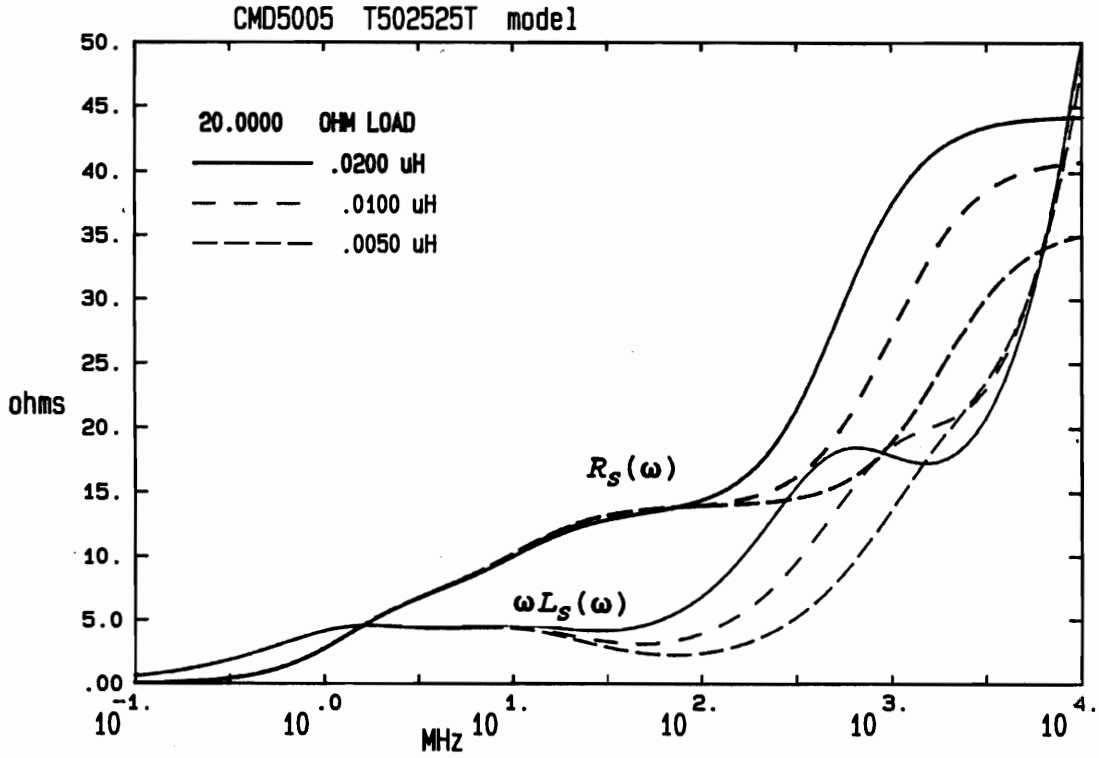

Figure 13. Analytical Model of CMD5005 T502525T FEB - 20 ohm.

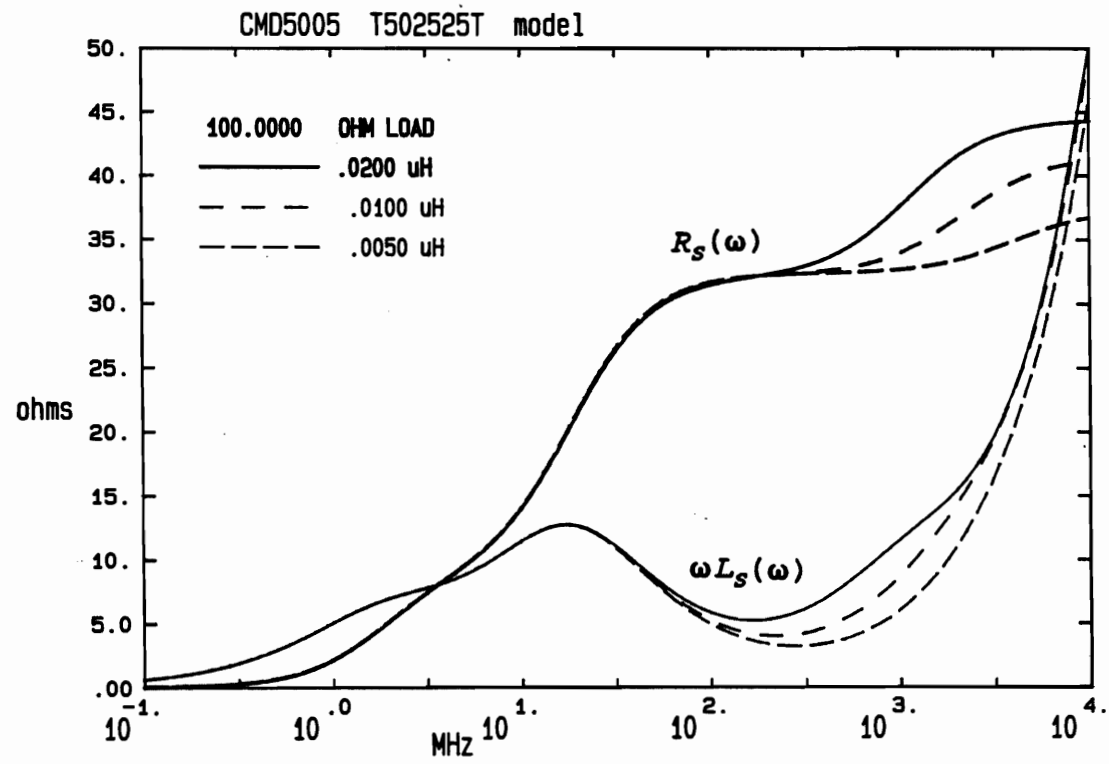

Figure 14. Analytical Model of CMD5005 T502525T FEB - 100 ohm.

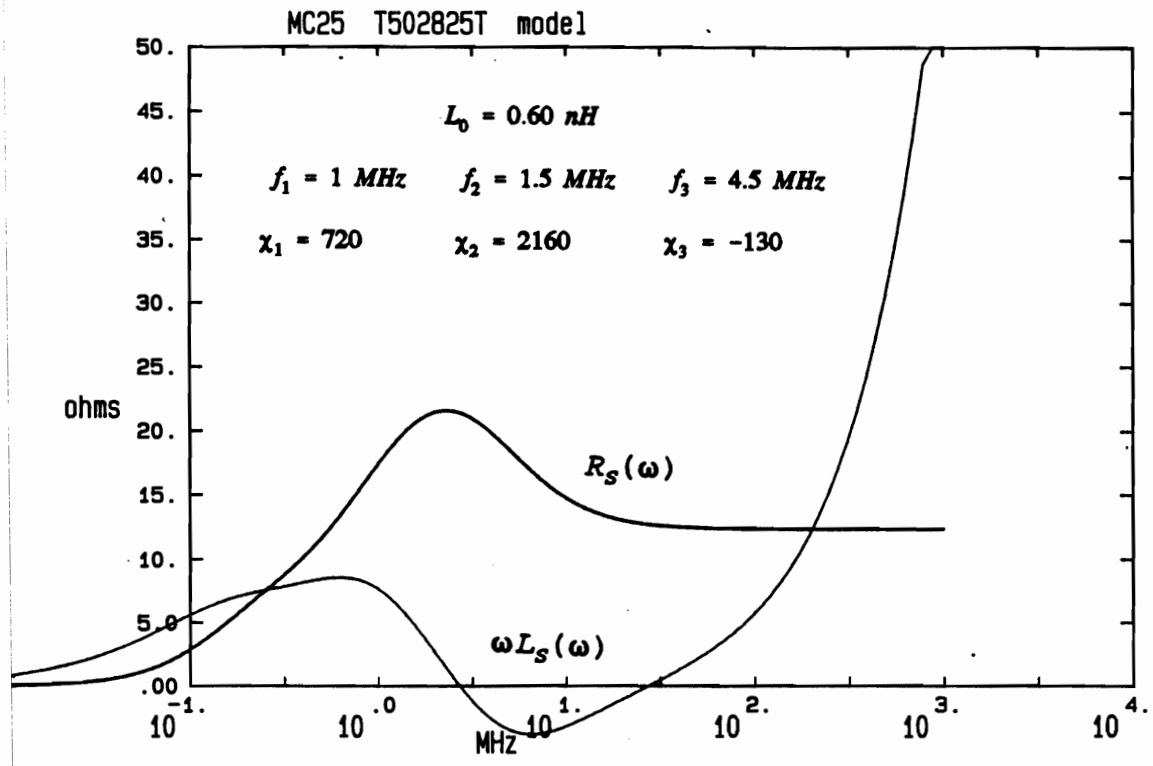

Figure 15. Analytical Model of MC25 T502825T FEB.

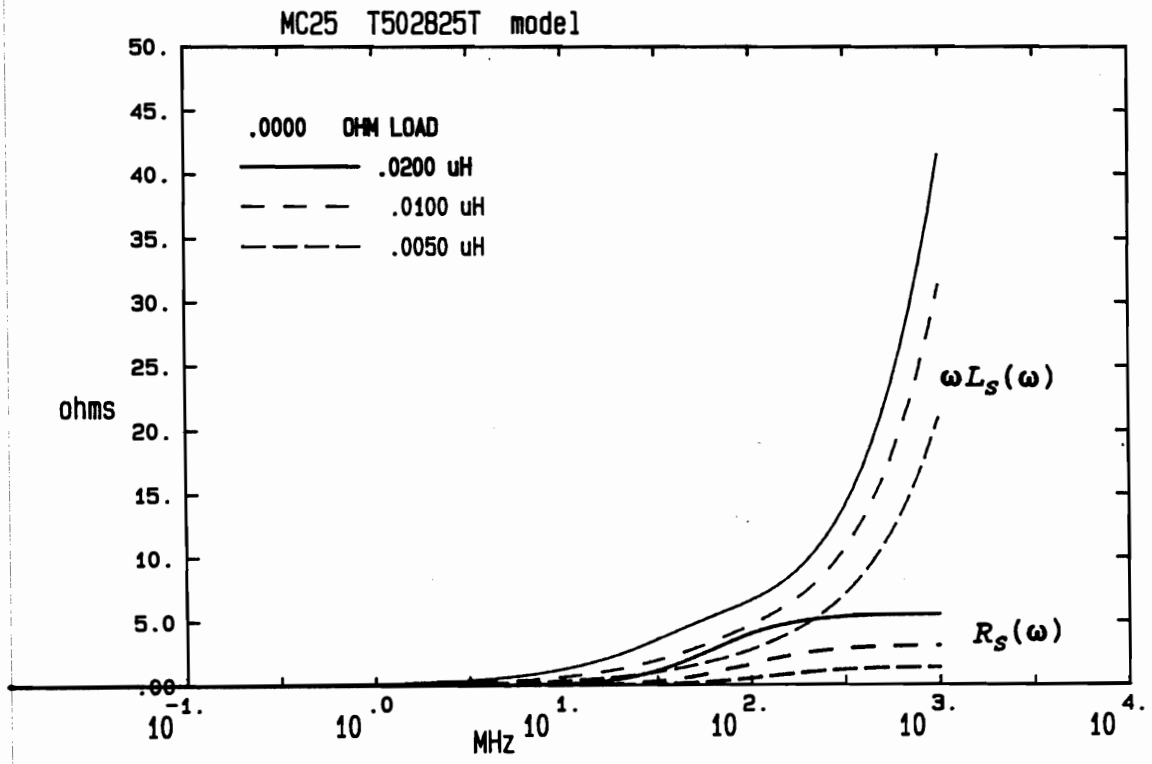

Figure 16. Analytical Model of MC25 T502825T FEB - short.

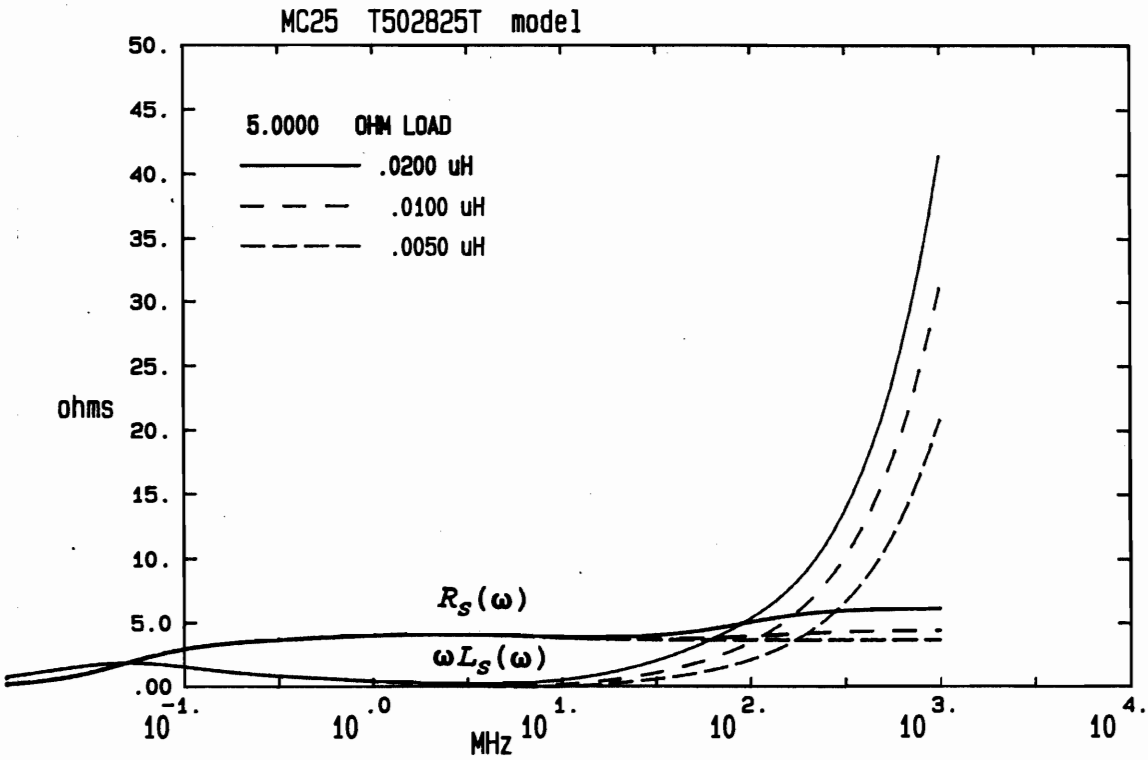

Figure 17. Analytical Model of MC25 T502825T FEB - 5 ohm.

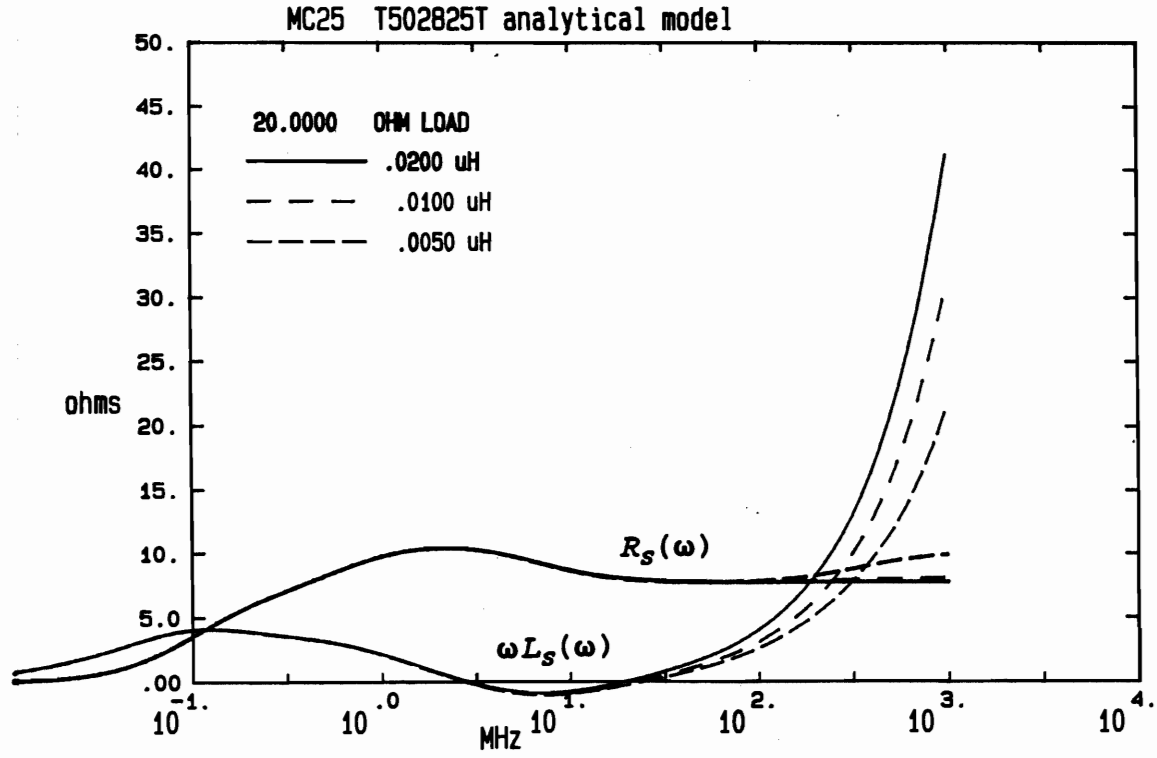

Figure 18. Analytical Model of MC25 T502825T FEB - 20 ohm.

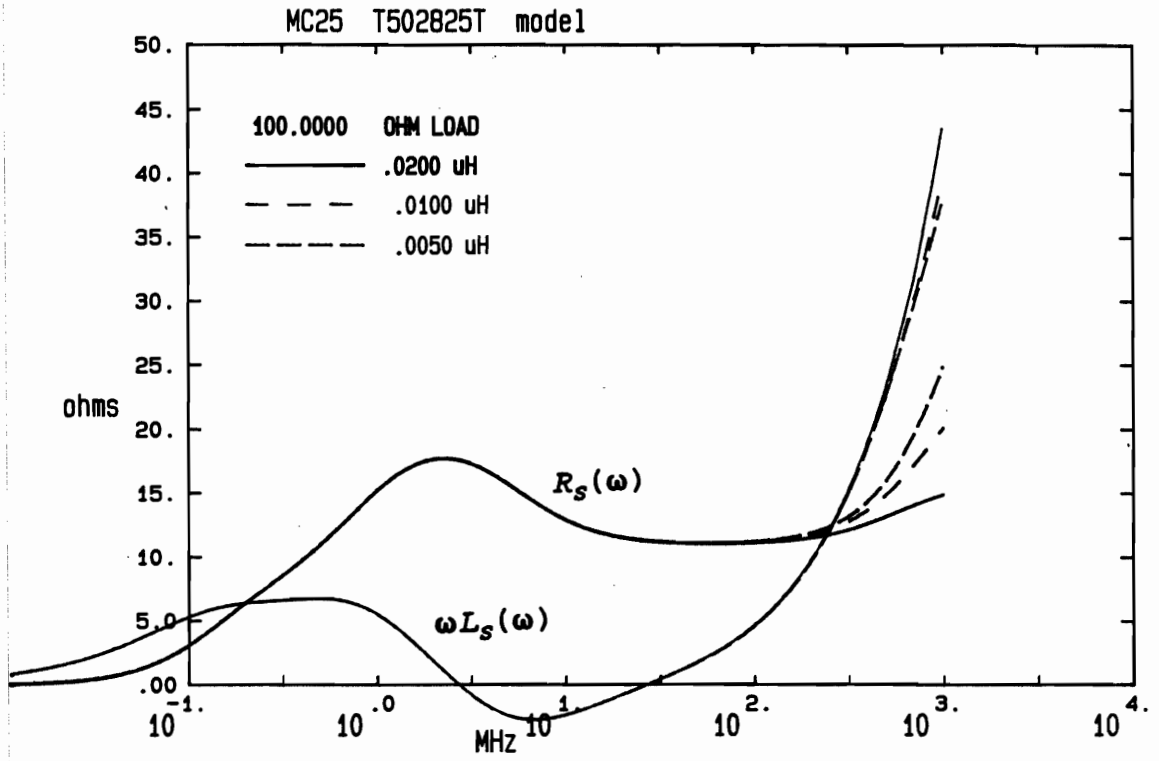

Figure 19. Analytical Model of MC25 T502825T FEB - 100 ohm.

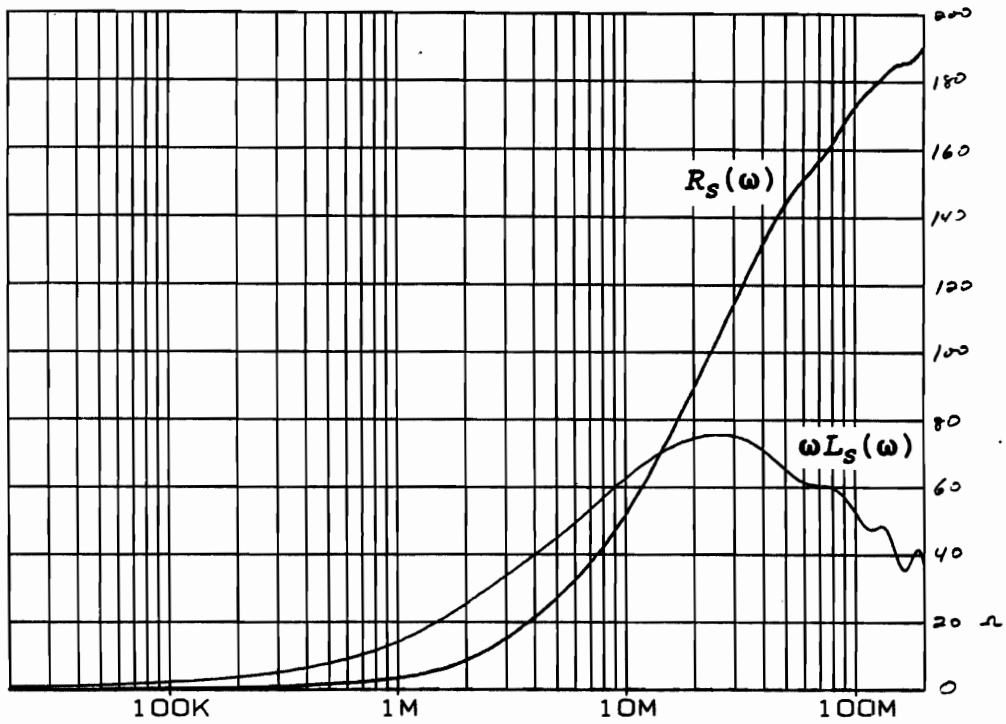

Figure 20. FB43-1020 Toroid FEB Impedance.

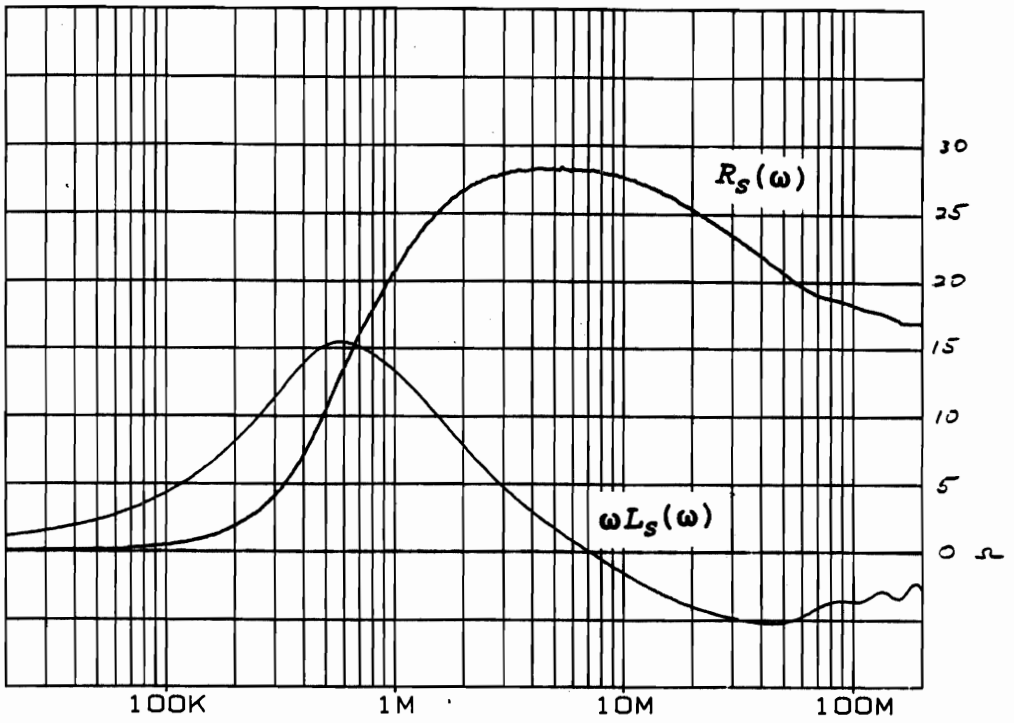

Figure 21. FB77-1024 Toroid FEB Impedance.

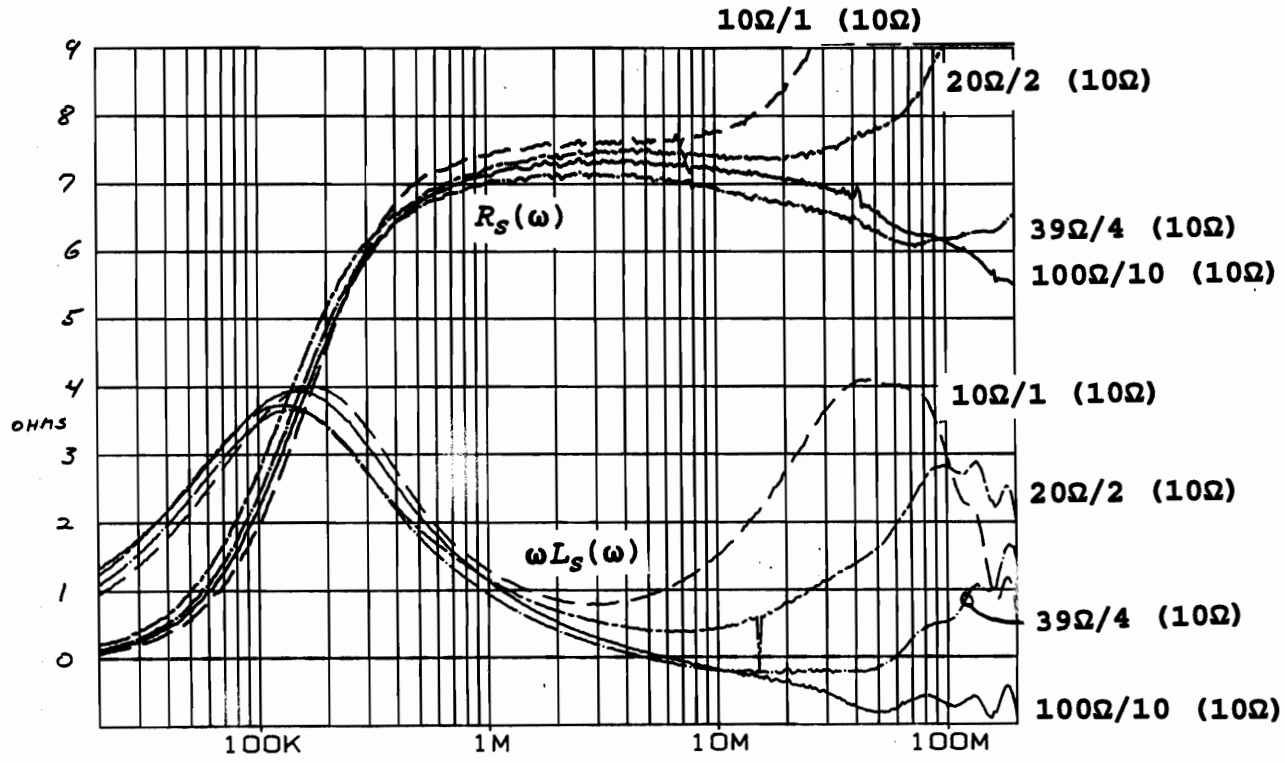

Figure 22. Loading of FB77-1024 FEB with Parallel Resistors: <u>10 OHM</u> Load Resistance, Varying Inductance.

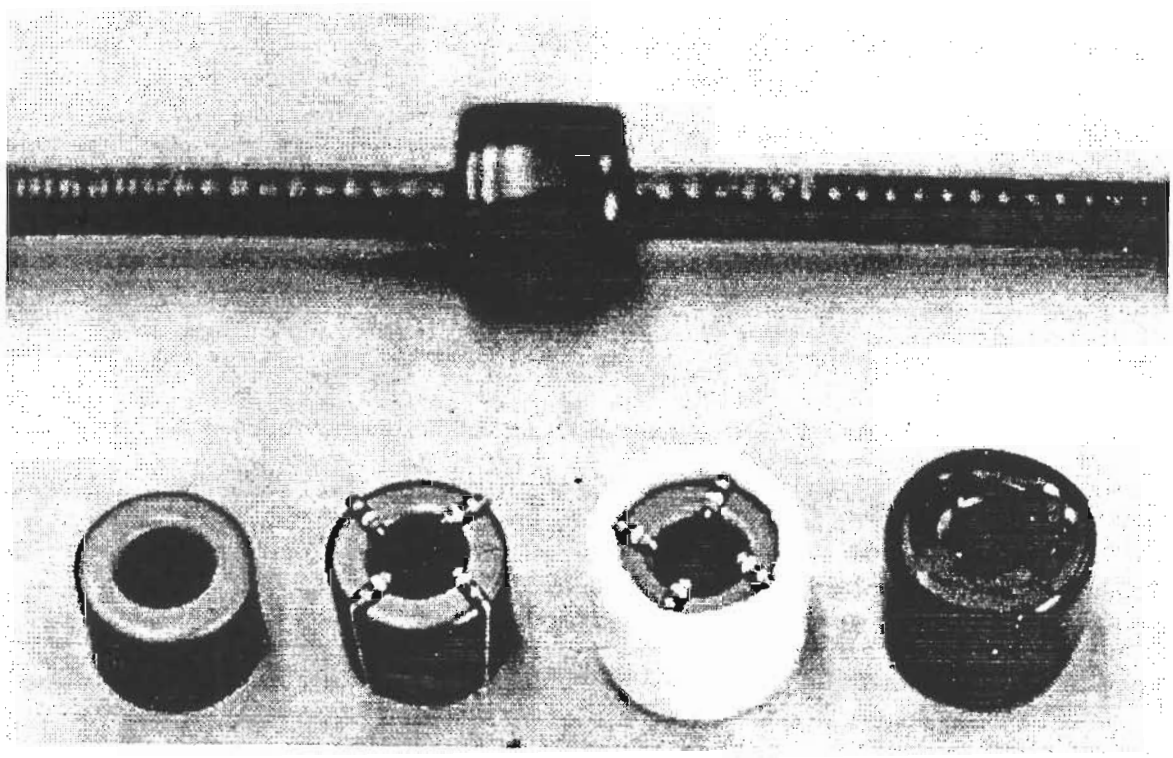

Figure 23. Details of Resistively-Loaded FEB Configuration:

- Bare toroidal FEB.
- FEB with Four 39 ohm resistors.
- Wound with Foam Tape.
- Covered with UV-Resistant Heat Shrink.
- Placed on Heliax Coaxial Cable (Positioning Tie-Wraps not Shown).

REFERENCES

1. C. E. Baum, W. P. Prather, and D. P. McLemore "Topology for Transmitting Low-Level Signals from Ground Level to Antenna Excitation Position in Hybrid EMP simulators," Sensor and Simulation Note 333, September 1991.

2. W. S. Kehrer, "ATHAMAS I Antenna Resistive Loading," ATHAMAS Memo 7, July 1975.

3. C. Zuffada, F. C Yang, and I. Wong, "On the Thin Toroidal and Elliptical Antennas," Sensor and Simulation Note 315, January 1989.

4. A. J. Dekker, Solid State Physics, Prentiss Hall, 1962.

5. E. A. Guillemin, Mathematics of Circuit Analysis, MIT Press, 1949.

6. N. Baladanian, T. A. Bickert, and S. Seshu, Electrical Network Theory, Wiley, 1969.

7. T. Sato and Y. Sakai, "Physical Meaning of Equivalent Loss Resistance of Magnetic Cores," IEEE Trans. Magnetics, p2894, Vol. 26, No. 5, September 1990.

8. J. Baker-Jarvis, R. G. Geyer, and P. D. Domich, "A Nonlinear Least-Squares Solution with Causility Constraints Applied to Transmission Line Permittivity and Permeability Determination," IEEE Trans. Inst. and Meas., p646, Vol 41, No. 5, October 1992.